Classification of Equilibrium Configurations of Wetting Films on Planar Substrates

Alexander V. Neimark* and Konstantin G. Kornev†

TRI/Princeton, 601 Prospect Avenue, Princeton, New Jersey 08542-0625

Received February 24, 2000. In Final Form: May 2, 2000

We suggest a rigorous formulation of the problem of classification of equilibrium configurations of wetting films on solid surfaces and in pores taking into account capillary and adhesion forces. As example, cylindrical films and drops of a van der Waals liquid on planar substrates are considered. Rewritten as a dynamic system, the Derjaguin equation for equilibrium interfaces is analyzed in detail without numeric calculation of interfacial profiles, providing a simple way for understanding the different wetting regimes. This method allows us to enrich the arsenal of well-known explicit solutions responsible for clarifying such physical problems as wetting and dewetting, capillary condensation and desorption, imbibition and drainage, droplet formation, and foaming on inhomogeneous substrates and in pores.

1. Introduction

When a drop is placed on a solid substrate, it may either spread out into a thin film or take on an equilibrium shape and adhere to the surface. Looking within classical thermodynamics for the choice between these options, one has first to check the sign of the spreading coefficient, $S = \gamma_{dry} - \gamma_{ls} - \gamma_{lg}$, where γ_{lg} and γ_{ls} are the liquid/gas and liquid/solid interfacial tensions and γ_{dry} is the surface energy of unwetted (dry) solid.[1−3] The positive values of S correspond to the conditions of absolute, or complete wetting; with time, a uniform film covers the substrate entirely. If, however, the film thickness decreases to a submicrometer scale, one has to amplify classical thermodynamics by Derjaguin's *disjoining pressure*.[4,5] The disjoining pressure Π accounts for liquid−solid intermolecular interactions and is a univalent function of the film thickness h; $\Pi = \Pi(h)$. In the case of curved films, the disjoining pressure is assumed to be additive to the Laplace, or capillary pressure caused by the curvature of the liquid−gas interface. The disjoining pressure concept enables one to obtain expressions for contact angles formed by drops on different substrates, to study equilibrium shapes of liquid coatings, to analyze a variety of surface processes such as capillary condensation, dewetting, thin film hydrodynamics, etc.[5−13] Recent advances in nanotechnology have ignited an explosion of theoretical works, attempting the nanoscale description of capillary phenomena; among the latest papers published in 1999, see refs 14−26. Different configurations of liquid coatings and droplets have been studied using the concept of disjoining pressure or equivalent expressions for the liquid−solid interactions.[7−20,24−33] However, a comprehensive classification of possible configurations of liquid coatings is still lacking. In this Letter, we sketch a new approach that puts the problems of film and droplet patterning into a unified frame and present the complete classification of the equilibrium shapes for the van der Waals films on planar substrates. A detailed description of the proposed method with applications to more complex systems and thorough literature review will be presented elsewhere.

2. Method

Equilibrium shapes of liquid layers (droplet or film) are determined by the Derjaguin equation in the following form:[4−6]

* To whom correspondence may be addressed. E-mail: aneimark@triprinceton.org.

† Permanent address: The Institute for Problems in Mechanics, Russian Academy of Sciences, Prospect Vernadskogo, 101, Moscow, 117526, Russia.

(1) de Gennes, P. G. *Rev. Mod. Phys.* **1985**, *57*, 827.
(2) Leger, L.; Joanny, J. F. *Rep. Prog. Phys.* **1992**, 431.
(3) Ruckenstein, E. *J. Colloid Interface Sci.* **1996**, *179*, 136.
(4) Derjaguin, B. V. *Acta Phys.-Chim. URSS* **1940**, *12*, 181; *Kolloid Zh.* **1955**, *17*, 207; *Colloid Polym. Sci.* **1975**, *253*, 492.
(5) Derjaguin, B. V.; Churaev, N. V.; Muller, V. M. *Surface Forces*; Plenum Press: New York, 1987.
(6) Kheifets, L. I.; Neimark, A. V. *Multiphase Processes in Porous Media*; (Khimia, Moscow, 1982).
(7) Joanny, J. F.; de Gennes, P. G. *C. R. Seances Acad. Sci.* **1984**, *299II*, 279. Joanny, J. F. *J. Mec. Theor. Appl.* (Paris), Numero special, **1986**, 249.
(8) Teletzke, G. F.; Davis, H. T.; Scriven, L. E. *Rev. Phys. Appl.* **1988**, *23*, 989.
(9) Hirasaki, G. J. In *Interfacial phenomena in Petroleum Recovery*; Morrow, N. R., Ed.; Marcel Dekker: New York, 1991; pp 23−73.
(10) Brochard-Wyart, F.; di Meglio, J. M.; Quere, D.; de Gennes, P. G. *Langmuir* **1991**, *7*, 335.
(11) Brochard-Wyart, F.; de Gennes, P. G. *Adv. Colloid Interface. Sci.* **1992**, *39*, 1.
(12) Stărov, V. M. *Adv. Colloid Interface. Sci.* **1992**, *39*, 147.
(13) Kornev, K.; Shugai, G. *Phys. Rev. E* **1998**, *58*, 7606.
(14) Neimark, A. V. *J. Adhes. Sci. Technol.* **1999**, *13*, 1137.
(15) Anklam, M. R.; Saville, D. A.; Prud'homme R. K. *Langmuir* **1999**, *15*, 7299.
(16) Aveyard, R.; Clint, J. H.; Paunov, V. N.; Nees, D. *Phys. Chem. Chem. Phys.* **1999**, *1*, 155.
(17) Bauer, C.; Dietrich, S. *Phys. Rev. E* **1999**, *60*, 6919; **2000**, *61*, 1664.
(18) Bico, J.; Marzolin, C.; Quere, D. *Europhys. Lett.* **1999**, *47*, 220.
(19) Dash, J. G. *Rev. Mod. Phys.* **1999**, *71*, 1737.
(20) Gau, H.; Herminghaus, S.; Lenz, P.; Lipowsky, R. *Science* **1999**, *283*, 46.
(21) Kornev, K. G.; Neimark, A. V.; Rozhkov, A. N. *Adv. Colloid Interface Sci.* **1999**, *82*, 127.
(22) Lenz, P.; Lipowsky, R. *Phys. Rev. Lett.* **1998**, *80*, 1920.
(23) Ross, D.; Rutledge, J. E.; Taborek, P. *Science* **1999**, *278*, 664.
(24) Rejmer, K.; Dietrich, S.; Napiorkowski, M. *Phys. Rev. E* **1999**, *60*, 4027.
(25) Solomentsev, Yu.; White, L. R. *J. Colloid Interface Sci.* **1999**, *218*, 122.
(26) Starov, V. M.; Churaev, N. V. *Colloids Surf., A* **1999**, *156*, 243.
(27) Yeh, E. K.; Newman, J.; Radke, C. J. *Colloids Surf., A* **1999**, *156*, 137; **1999**, *156*, 525.
(28) Broekhoff, J. C. P.; de Boer, J. H. *J. Catal.* **1967**, *9*, 8; **1968**, *10*, 153; **1968**, *10*, 368.
(29) Saam, W. F.; Cole M. W. *Phys. Rev B* **1975**, *11*, 1086.
(30) Philip, J. R. *J. Chem. Phys.* **1977**, *66*, 5069.
(31) Neimark, A. V.; Kheifetz, L. I.; *Kolloidn. Zh. USSR* **1981**, *43*, 500.
(32) Ruckenstein, E.; Lee, P. S. *Surf. Sci.* **1975**, *52*, 298.
(33) Brochard, F. *J. Chem. Phys.* **1986**, *84*, 4664.

10.1021/la000267b CCC: $19.00
Published on Web 05/27/2000

$$-\frac{h''}{(1+h'^2)^{3/2}} = [P_{cap} + \Pi(h)]/\gamma_{lg} \quad (1)$$

Here, for the sake of simplicity, we limited ourselves to one-dimensional cylindrical configurations on a plane substrate. h(z) is the layer thickness as a function of the lateral coordinate z; $h' = dh/dz$ and $h'' = d^2h/dz^2$ are the first and second derivatives, respectively. The sum in the right-hand side of eq 1 consists of capillary pressure P_{cap}, which is the pressure difference in the liquid and gas, $P_{cap} = P_{liquid} - P_{gas}$, and disjoining pressure $\Pi(h)$. The Derjaguin equation (1) describes different configurations of liquid layers and droplets, which are specified by the imposed boundary conditions. However, it is instructive to pose the problem of a topological classification of possible geometrical shapes. Thus, the problem is reduced to the analysis of the following equivalent dynamic system:

$$h' = u, \qquad u' = -(1+u^2)^{3/2}[P_{cap} + \Pi(h)]/\gamma_{lg} \quad (2)$$

Here, we use the mathematical term "dynamic system" applied to equations describing an equilibrium since the system (2) can be treated as a vector field with components (h',u') schematically presented in Figure 1. Considering the streamlines of this field in the right semiplane $h > 0$, we can describe different shapes of the liquid layers. The vector field has stationary points located at the h-axis ($u = 0$). The stationary points fulfill the algebraic equation

$$-\Pi(h_{eq}) = P_{cap} \quad (3)$$

Equation 3 is merely the condition of thermodynamic equilibrium of a uniform film of zero curvature. Note, that the capillary pressure in eq 1 is defined as the pressure difference in the liquid and gas phases and, thus, is not necessarily associated with the film curvature.

We restrict ourselves to monotone decreasing isotherms of the disjoining pressure such as $\Pi(h) = A_n/h^n$. If $n = 3$, we deal with the van der Waals film for which A_{vdW} is the effective Hamaker−Lifshitz constant.[1] The positive value of the Hamaker−Lifshitz constant implies that we deal with the situation of complete wetting.[1,4,9−12] For monotone decreasing isotherms, eq 3 has a unique solution for negative capillary pressures; in this case, the system (2) has one stationary point. For positive capillary pressures, no solutions of eq 3 and subsequently no stationary points of the system (2) exist. This means that in the uniform wetting film, the liquid pressure cannot exceed the gas pressure. The dynamic system (2) has a singular line $h = 0$, because the disjoining pressure isotherm diverges as the film thickness diminishes. Keeping the problem of its validity beyond the scope of this Letter (see, i.e., discussion in ref 3), we, nevertheless, formally analyze the dynamic system (2) in the entire semiplane $h > 0$. However, the solutions obtained are physically meaningful only above a lower cutoff of film thicknesses which must exceed at least one molecular diameter.

The phase portraits of the system (2) are depicted in Figure 1; the windows (a) and (b) correspond to negative and positive capillary pressures, respectively. An analysis of the system (2) in the vicinity of the stationary point (h_{eq},0) shows that the point is hyperbolic. There are four separatrices which emanate from or arrive at the stationary point (h_{eq},0); see Figure 1a. The separatrices demarcate three qualitatively different classes of solutions to eqs 2 at the given capillary pressure. The first class contains the streamlines, which lie between the line $h = 0$ and the left separatrices. The second class includes the V-shaped streamlines situated between the left and right separatrices. As seen from eqs 2, the V-shaped stream functions $u(h)$ have a minimum in the upper quadrant and a maximum in the lower at $h = h_{eq}$. The third class consists of the streamlines bounded by the right separatrices. Except for the separatrices, the streamlines which intersect the axis $u = 0$ form with it a right angle. For positive capillary pressures (Figure 1b) no stationary point exists, and the stream functions $u(h)$ decrease in the upper quadrant and increase in the lower. All streamlines have vertical asymptotes as $u \to \pm\infty$ that correspond to the vertical inclination of the film profile with respect to the substrate plane. This is a specific feature of the solutions of Derjaguin's eq 1.

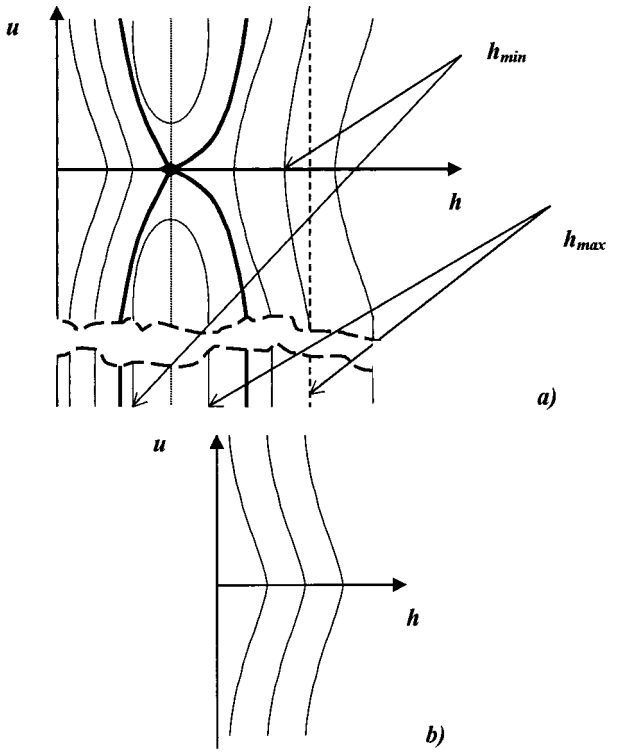

Figure 1. Phase portrait of the system (2): (a) for negative capillary pressure; (b) for positive capillary pressure. The separatrices are boldface; the hyperbolic point is denoted by the symbol ◆.

In the earlier literature, considerable attention has been paid to configurations of wetting films on surfaces and in pores which were studied by direct solution of eq 1 employing its first integral.[1−14,24−31] However, the considerations were restricted to infinite and energetically uniform substrates and pore walls. Therefore, the configurations included only equilibrium menisci transiting into infinite films[4] and planar droplets with sharp edges,[32] or pancakes.[7] As we show below, the infinite configurations of menisci and pancakes correspond to the separatrices depicted in Figure 1a). A variety of other streamlines correspond to liquid configurations on finite size substrates and reflect the effects of the film pinning which may occur, for example, at the substrate edges. Similar pinning occurs at the boundaries between liophilic and liophobic patches of a heterogeneous substrate.[17,18,20,22]

3. Classification of the Equilibrium Shapes for the Van der Waals Films on Planar Substrates

Infinite Uniform Film. The stationary point corresponds to the equilibrium uniform film (Figure 2a) of thickness h_{eq} determined from eq 3.

Meniscus Transiting into the Infinite Film. The right separatrices describe menisci of bulk liquid being in

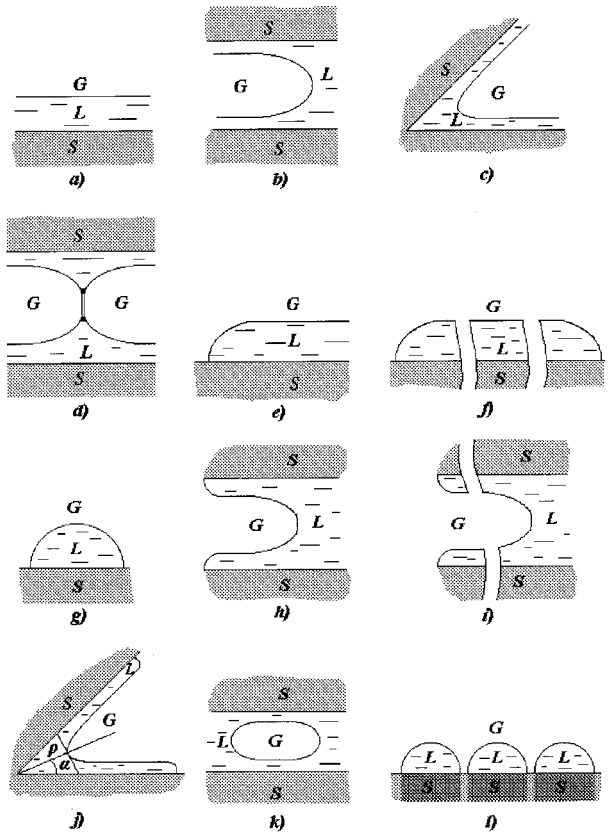

Figure 2. Schematic configurations of liquid films and droplets allowed by the Derjaguin model: (a) uniform film; (b) meniscus in an infinite slit-shaped pore transiting into the uniform film; (c) meniscus in an infinite wedge-shaped pore transiting into the uniform film; (d) plateau border between the wetting films on the pore walls and the foam lamella in the pore cross section; (e) edge of a semi-finite film; (f) macroscopic pancake; (g) microdroplet; (h) meniscus pinned at the pore mouth; (i) meniscus in a finite slit-shaped pore; (j) meniscus in a finite wedge-shaped pore; (k) bubble in a pore; (l) pinned droplets, on liophilic patches of a heterogeneous substrate.

equilibrium with uniform infinite films. These menisci can be realized in narrow pores in the processes of capillary condensation, evaporation, drainage, imbibition, and forced gas−liquid displacement. Since we are restricted by plane substrates, the right separatrices in Figure 1a) describe the profile of the transition zone between menisci and wetting films in slit-shaped (Figure 2b) and wedge-shaped (Figure 2c) pores, and also the configuration of the Plateau border (Figure 2d) between the wetting film on the pore walls and the foam lamella in the pore cross section.[13] The right separatrices have vertical asymptotes as $u \to \pm\infty$ and $h \to H/2$, where H is the width of the pore in which capillary condensation occurs at the given capillary pressure P_{cap}. The relation between the pore width and the pressure of capillary condensation, $P_{cap} = P_t(H) \approx (\gamma/H)(1 + O(h_{eq}/H))$, is determined by the Derjaguin equation, which follows from the first integral of the eq 1.[4] The analytical solution for the equilibrium profile of the transition zone, which corresponds to the right separatrices, was derived earlier in ref 31. It was shown that the characteristic length of the transition zone is of the order of $l_{trans} \propto (Hh_{eq})^{1/2}$.

Semi-infinite Films, Edges, and Macroscopic Pancakes. The left separatrices correspond to semi-infinite films with the right (the upper left separatrix) and left (the lower left separatrix) edges (Figure 2e). For the sake of brevity, we will call these configurations "edges". A macroscopic pancake (Figure 2f) can be constructed by two edges (left separatrices) connected by the uniform film (stationary point). Determined solely by the spreading coefficient S, the equilibrium pancake thickness h_{eq} is calculated from the condition of minimum of the excess free energy at given constant drop volume:[1,3,7,10,32] $S = \int_{h_{eq}}^{\infty} \Pi(h)\, dh + h_{eq}\Pi(h_{eq})$. The edge shape is determined by eq 1. The Laplace force plays an important role only at the pancake edge providing a continuous transition of the drop profile from the flat film surface to the substrate. It is worth noting that the profile of the pancake edge has been studied earlier[1,2,7,9] in the approximation of smooth profiles. This method implies that the profile curvature in the left-hand side of eq 1 is approximated by the second derivative d^2h/dz^2, which is reasonable for slightly curved interfaces but does not capture the sharp bend of the film profile at the edge. An analysis of the phase portrait of the system (2) shows that the solution of eq 1 at the film edge necessarily implies the film approaching the substrate at a right angle which is achieved at a finite film thickness h_{edge}; $u = dh/dz \to \pm\infty$ at $h \to h_{edge} > 0$, where h_{edge} is determined from the algebraic equation $S + \gamma = \int_{h_{edge}}^{\infty} \Pi(h)\, dh + h_{edge}\Pi(h_{edge})$. For the van der Waals films $h_{eq} = (3\gamma/2S)^{1/2}a$, and $h_{edge} = (3\gamma/2(S+\gamma))^{1/2}a = (S/(S+\gamma))^{1/2}h_{eq}$ with $a = (A/\gamma)^{1/2}$ being a characteristic molecular length.[7] Choosing as a typical example $S/\gamma = 10^{-2}$, we see that while the pancake thickness is of the order of 10 molecular diameters, the edge thickness is comparable with the monolayer thickness. In fact, h_{edge} gives an estimate for the lower cutoff of applicability of the continuum approach, eq 1. To clarify the geometry of the film edge with subnanometer resolution, one has to apply molecular level models. An analysis of the pancake profile at the pancake top, $h \to h_{eq}$, gives the asymptote $(h_{eq} - h) \propto \exp(-z/l_p)$ with the characteristic scale $l_p \propto h_{eq}^2/a \propto (\gamma/S)a$. This picture of macroscopic pancakes fails in the case of microdroplets of width smaller than l_p, when the opposite pancake edges start to "fill" each other and the edge effects overlap. For $S/\gamma = 10^{-2}$, this characteristic width is estimated as hundred molecular diameters.

Mircodroplets, or Pancakes of Finite Size. The set of streamlines located in the region bounded by the singular line $h = 0$ and the left separatrices correspond to 2D striplike microdroplets (Figure 2g), the maximum height of which is smaller than the thickness of the equilibrium film, h_{eq}. Starting from plus infinity at the left top of Figure 1a), $u \to +\infty$, in the upper quadrant the trajectories are decreasing functions of the film thickness. The inequality $h'' = du/dx = (du/dh)u \neq 0$ holds everywhere, and therefore the microdroplets have no valleys or steps. The streamlines are distinguished by their vertical asymptotes as $u \to \pm\infty$. This means that the profile edge necessarily approaches the substrate at a right angle and the minimum film thickness at the edge is finite. This situation is similar to the pancake edge described above. Thus, the continuum eq 1 implies that the theoretical profile of a microdroplet ends abruptly with the prescribed right inclination angle, ±90°. Although it is tempting to make a conclusion that all films must form with the dry substrate the microscopic contact angle of 90°, we cannot treat the film edge inclination angle as a contact angle since the continuum approach is inapplicable to films of thickness comparable with the molecular length.[3] Microdroplets with overlapping edge effects can be realized on surfaces of nanostructured solids, in particular, on liophilic patches of heterogeneous surfaces when the patch size is smaller than the characteristic pancake width $l_p \propto h_{eq}^2/a \propto (\gamma/S)a$.

Menisci Transiting into Precursor or Left-Behind Films. The streamlines located between the left and right separatrices describe configurations of transition zones between finite length films and menisci. Therewith, the film minimal thickness h_{min} corresponds to the vertical asymptote as $u \rightarrow +\infty$, $h < h_{eq}$, and the height of the meniscus cupola, h_{max}, corresponds to the vertical asymptote as $u \rightarrow +\infty$, $h > h_{eq}$. The finite length films are usually referred to as precursor films in the processes of meniscus advancement or left-behind films in the processes of meniscus receding. Remarkably that similar to the pancake edge, the edge of the precursor/left-behind film approaches the substrate surface at a right angle and again there is a cutoff as the film thickness reaches the minimal thickness h_{min}. These solutions allow us to extend the theory of capillary condensation taking into consideration the edge effects. In previous works on capillary condensation the finite length film configurations have not been taken into account since the authors considered the meniscus in equilibrium with infinitely long uniform film.[4,24,28−31] This solution is exceptional and corresponds to the right separatrices. The trajectories under consideration correspond to the family of equilibrium menisci in slit pores (the pore width equals $H = 2h_{max}$) transiting into finite length films pinned at the pore mouth (Figure 2h). Thus, these solutions describe the process of gradual receding of the meniscus cupola into the pore as the pressure difference decreases. While the pressure difference is small, the meniscus is located at the pore mouth. As the pressure difference increases the meniscus is displaced inside the pore, but the edge of the left-behind film retains its position at the pore mouth. When the depth of the meniscus penetration exceeds h_{eq}^2/a, the meniscus approaches the shape corresponding to the right separatrix. At the pore mouth the pancake-like construction can be applied. The only modification is that the film edge is pinned at the pore wall end and the uniform film is continuously transformed into the meniscus. The limiting configuration (Figure 2i) is formed by the right separatrix transiting into the left separatrix. A similar scenario of condensation/evaporation can be applied to the menisci in finite wedgelike pores (Figure 2j). The above analysis shows that, instead of abrupt pore filling/emptying at $P_t(h)$, the condensation/evaporation is a gradual process associated with the precursor/left-behind film formation and development. This effect leads to smoothing the stepwise capillary condensation−desorption hysteresis isotherms implied by classical theories. The finite size effects are of special importance in the vapor sorption and evaporation in nanoporous materials with pores of 2−200 nm in diameter including silica gels, porous glasses, mesoporous molecular sieves, pillared clays, and carbon nanotubes among the others. It is worth noting that the initial eq 1 is justified when the pore width sufficiently exceeds the equilibrium film thickness, $H = 2h_{max} \gg 2h_{eq}$. An analysis based on the density functional theory shows that this strong inequality implies typically a 3-fold difference.[34] Otherwise, the potentials imposed by the opposite pore walls overlap.

Confined Bubbles. The trajectories of the region bounded by the right separatrices differ significantly from the others. They cross the axis $u = 0$. At this point the film thickness is minimal, h_{min}, and its profile has a zero inclination angle. At the same time, all streamlines go to infinity, $u \rightarrow \pm\infty$. This implies that the interface profile also has two points, at which the profile indentation is maximal, h_{max}, and the inclination angle achieves its limiting values of $\pm 90°$ which correspond to the meniscus cupolas. These trajectories describe configurations of confined bubbles (Figure 2k) or bubble trains in the slit-shaped pores. For the latter, each pair of bubbles is separated either by a lens or by a foam lamella sketched in Figure 2d). The family of bubbles can be formed at the given capillary pressure P_{cap} in the pores of different width $H = 2h_{max}$. Therewith, the range of permissible pore widths is limited by the asymptote of the right separatrix $H_c(P_{cap})$ from below. As h_{min}, h_{max}, and subsequently H increase, the bubble configuration approaches the cylindrical bubble of radius $h_{max} - h_{min} = -\gamma/P_{cap}$, which would be formed in the bulk liquid. Note, that although all configurations corresponding to the solutions of eq 1 are equilibrium, their stability must be determined from energetic considerations, a problem which is beyond the scope of this communication.

Pinned Droplets. Turning now to the case of positive capillary pressures (Figure 1b) and applying similar analysis, one can be convinced that the only admissible film configuration is a convex cylindrical droplet (Figure 2l). In contrast with microdroplets (Figure 1g), in which the adhesion forces dominate so much that the capillary pressure is negative, here the surface tension forces shape the droplet body except for its edges. The same reservations as before must be made about the applicability of the employed approach to the description of the droplet configuration in the vicinity of the pinning line. The configurations under consideration can be realized on a patchy striped substrate where the width of the liquid droplet is controlled by the width of the hydrophilic stripe. Even wetting, the liquid is unable to spread over the whole substrate, because the latter is essentially hydrophobic. So, the film inevitably bulges to take on a curved cylindrical shape with the edges pinned at the stripe borders.[17,18,20,22] As the minimal thickness h_{min} increases, the trajectories in Figure 2l approach the trajectory corresponding to the circular droplet shape of which is unaffected by the substrate.

In summary, the results presented in this Letter constitute the idea of a unified theory of wetting and spreading based on Derjaguin's equation of capillarity. For now, only particular solutions of the Derjaguin equation, limited to infinite substrates, were considered. We showed that the arsenal of allowed solutions to this equation is rich and depends significantly on the substrate geometry and adhesion potential. The phase portrait method enables one to enrich the existing class of equilibrium solutions and take into account the finite size effects. Rigorous mathematical formulation is outlined for the description of the wetting film configurations at the nanometer scale, including film edges, pancakes, pinned droplets, menisci, lamellae, and confined bubbles. The analysis of phase portraits gives also the mathematical limits of applicability of the Derjaguin equation to the van der Waals films.

Acknowledgment. This work was supported by a group of TRI corporate participants.

LA000267B

(34) Ravikovitch, P. I.; Neimark, A. V. *Stud. Surf. Sci., Catal.* **2000**, *129*, 597.